JOURNAL OF MATERIALS SCIENCE 18 (1983) 1297–1305

Is bone a Cosserat solid?

HYO SUB YOON, J. LAWRENCE KATZ
Department of Biomedical Engineering, Rensselaer Polytechnic Institute, Troy, New York 12181, USA

In a viscoelastic composite material including bone, acoustic waves undergo both geometric and viscoelastic dispersions as they propagate through the medium. The viscoelastic dispersion is characterized by an increase in phase velocity with increase in frequency, while the geometric dispersion is well-known. By comparing the dispersion data on these and other types of materials, it has been noted that the increases in the ultrasonic velocities for bones are much larger than those for simple viscoelastic solids and composites, suggesting an additional dispersion mechanism. This additional dispersion can be explained by Mindlin's theory on the Cosserat continuum with microstructure.

1. Introduction

When there is a geometrical discontinuity in a structural member or a machine part, such as a hole and a notch, a stress concentration (stress raiser) occurs at the discontinuity. In orthopaedic surgery, screw holes or other types of discontinuity are often introduced into a bone. The stress concentration is expressed by a theoretical stress-concentration factor which is the ratio of the maximum stress to the nominal stress, and which can be calculated from the theory of classical elasticity. It is generally known that the apparent fatigue and fracture strengths of some materials are affected by strain gradients. In bending fatigue tests, the smaller the specimen or grain size, i.e. the higher the strain gradient across the specimen, the higher the fatigue limit or strength. Also fractures in brittle materials and the onset of static yielding in ductile materials in the presence of stress concentration, occur at higher loads than might be expected on the basis of the stress-concentration factor [1–3].

These results suggest the need for an extension of the theory of elasticity to include strain gradients. The simplest extension is the well-known Cosserat theory [4] where an additional force-like quantity, couple-stress (couple per unit area), is taken into account in addition to the usual stress or force-stress (force per unit area) of classical elasticity. Just as strain is associated with stress, so the rotation gradient, curvature, is associated with couple-stress. According to Mindlin [5], in the linear Cosserat theory for an isotropic elastic material, there is an additional modulus of elasticity with dimensions of force, the ratio of couple-stress to curvature or twist, i.e. a modulus of bending and twisting. The square root of this bending-twisting modulus to the usual shear modulus has the dimension of length. This length, l, is a material property which characterizes the entire difference between analogous equations or solutions with and without couple-stress. The larger l may be, the greater is the difference. In single crystals and amorphous materials such as glasses or plastics, l is probably submicroscopic; it might be of the order of the radius of the root of a crack. In polycrystalline or granular materials or generally in any material with microstructure, l may be considerably larger. Based on the Cosserat or couple-stress theory, Mindlin [5] has also recalculated the stress-concentration factors around a circular hole in two dimensions. His results show that, both in a field of simple tension and in a field of pure shear, the stress-concentration factors depend on both Poisson's ratio and the ratio of the radius, r, of the hole to the material constant, rather than being the usual constant values 3 and 4, respectively. As r/l decreases, so does the stress-concentration factor.

Koiter [6] suggested three simple but crucial tests for the numerical determination of the

0022–2461/83 $03.00 + .12

additional elastic constants l and η (a non-dimensional number similar to Poisson's ratio) in an isotropic material: 1. torsion of a cylindrical bar; 2. cylindrical bending of a rectangular plate; and 3. pure bending of a rectangular beam. In his experiment on aluminium alloy (2014-T3) using Method 3, Schijve was unable to detect an influence of couple-stresses on the stress concentration [7]. Employing Method 2, Ellis and Smith [8] have investigated both annealed and cold-worked pure aluminium sheets and annealed low-carbon steel sheets. They concluded that couple-stress effects would not be revealed until the plate thickness approaches grain size, and that under such conditions, the continuum theory will break down. Gauthier and Jahsman [9] also reported on their unsuccessful attempt to detect "non-classical" effects from static torsion experiments on aluminium-epoxy composite cylinders, interpreting that the effects were masked by material inhomogeneity. On the other hand, Perkins and Thompson [10] have shown that the apparent shear modulus of an elastic cylinder bonded to inner and outer rigid cylinders appears to follow the theoretical curve based on the linear elastic couple-stress theory [11] and on additional assumptions. A closed-cell polyvinyl chloride foam was used as the elastic medium and the couple-stress constant l was set equal to the average value of the cell diameter of the foam as determined by optical measurements. The apparent shear modulus was determined from the measured resonant frequency of the system. Also, Yang and Lakes [12–14] reported on the determination of the characteristic length l' $(= l(1+\eta)^{1/2}) = 0.14\,\text{mm}$ for human femoral compact bone, which appears to be more convincing evidence of the couple-stress effects. In addition, their results on polymethyl methacrylate (PMMA) with the same experimental set-up, show that PMMA behaves classically.

Although several interesting theoretical studies have been reported on wave propagation in a generalized continuum, there have been no experimental investigations, particularly on ultrasonic wave propagation, as far as these authors are aware (except for the present investigation). For a linear isotropic Cosserat continuum, Mindlin and Tiersten [11] have shown that there is a non-dispersive dilatational wave, as in the usual theory, propagating at the usual velocity. However, there are now two rotational waves: one propagating and the other non-propagating. Both rotational waves are dispersive. The group velocity of the propagating rotational wave increases with increasing wave number (or frequency) and increasing l. The non-propagating wave produces a boundary layer effect. On the other hand, in a linear elastic solid with microstructure (Mindlin [15]) both longitudinal and transverse velocities increase with increasing wave number. Parfitt and Eringen [16] have found that in an infinite isotropic "micropolar" elastic solid, there exist four types of waves propagating with four distinct speeds: v_1 and v_2 (longitudinal), and v_3 and v_4 (transverse). Of the last three dispersive types (v_2, v_3, v_4), v_2 and v_3 (or squared velocities in their expressions) *decrease significantly*, but v_4 increases slightly, with increasing frequency $(\omega = 0 \to \infty)$.

In order to place the present study in proper perspective, and at the same time complement this Introduction, a short historical review of generalized continuum theories is presented in Section 2. However, this is not intended to be a critical review. Since there appears to be some evidence of couple-stress effects in bone, as mentioned previously, the linear elastic Cosserat theory [11] is summarized in the first part of Section 3, emphasizing the effects of couple-stresses on plane wave propagation. Also in Section 3 is included a brief summary of the theory of linear elasticity with microstructure [15], which seems to describe more satisfactorily than does the Cosserat theory the experimental data on ultrasonic velocities in human bones.

2. Historical review of generalized continuum theories

Since the literature on the generalized continuum theories is enormous, this review is intended to be as brief as possible, and is mainly concerned with some of the highlights closely related to the present paper.

In his unfinished work, Poisson (1842) made an attempt to include directionally dependent "molecular" interactions in the elastic potential energy [17, 18]. Cauchy (1851) first extended the continuum theory to accommodate short wavelengths, consequently effects of the atomic structure of solids. His work would, if completed, correspond to the inclusion of all the gradients of strain, in addition to the strain, in the potential energy density [19]. The couple-stress theory

initiated by Voigt (1887) [20, 21] has been elaborated by the Cosserat brothers (1909) [4], whereas Duhem (1893) considered a volume element or unit cell as a collection not only of points but also of directions associated with the points [22]. The corner singularity which exists in the absence of couple-stresses, was noted by Reissner (1944) [23].

Ericksen and Truesdell (1958) developed further the purely kinematic description of the Cosserat continuum, emphasizing the one- and two-dimensional cases of rods and shells, without exploring the theory of the motion of the continuum [24]. Günther (1958) related his study on the kinematics and statics of the three-dimensional Cosserat continuum to dislocation theory [25]. In 1960 there appeared several modern derivations of the couple-stress theory; Rajagopal [26], Truesdell and Toupin [27], Aero and Kuvshinskii [28], and Grioli [29]. This so-called "Cosserat theory with constrained rotations" [30] takes into account the first gradient of rotation, i.e. eight of the eighteen components of the first strain gradient. Schaefer (1962) solved several explicit boundary value problems for a two-dimensional Cosserat medium so as to illustrate some of the novel features of the theory [31]. Toupin (1962) developed the complete first strain gradient theory in a nonlinear form [32]. At the same time, Mindlin and Tiersten (1962) [11] have linearlized Toupin's constitutive equations and solved a number of problems in the linear theory of elasticity with couple-stresses, e.g. wave propagation, vibration, stress functions, nuclei of strain, and others. In addition, they showed the interrelationships among the different derivations of the Cosserat equations by Aero and Kuvshinskii [28], Grioli [29], and Toupin [30]. Mindlin (1964) [15] formulated a linear theory of a three-dimensional elastic continuum which has some of the properties of a crystal lattice as a result of the inclusion of the idea of the unit cell into the theory. The mathematical model of a microvolume element or cell is a linear version of the deformable directors of Ericksen and Truesdell [24]. If the cell is made rigid, the equations reduce to those of a linear Cosserat continuum [4]. Eringen and Suhubi (1964) introduced a general theory of a nonlinear "microelastic" continuum in which the balance laws of continuum mechanics are supplemented with additional ones, and the intrinsic motions of microelements contained in such macrovolume are taken into account [33, 34]. Green and Rivlin (1964) have established the basis of a very general theory which includes strain-gradients of any orders [35, 36], which they call "multipolar continuum mechanics".

Additional references are given in Tiersten and Bleustein (1974) [37], Eringen (1968) [38], and more recent articles on generalized continua.

3. Theoretical background

3.1. Linear elastic couple-stress theory [11]

In summarizing the work of Mindlin and Tiersten, their dyadic or polyadic notation will be used [39, 40].

3.1.1. The Cosserat equations

Consider the motion of a portion of a material volume V, bounded by a surface S with outward normal $\mathbf{n}$. Across S there act force-stress and couple-stress vectors, $\mathbf{t}_n$ and $\mathbf{m}_n$, while within V there act body-force and body-couple vectors, $\mathbf{f}$ and $\mathbf{c}$. The equations for the conservation of mass, balance of linear and angular momenta, and conservation of mechanical energy are, respectively, expressed by:

$$\frac{\mathrm{d}}{\mathrm{d}t}\int_V \rho \mathrm{d}V = 0 \tag{1}$$

$$\frac{\mathrm{d}}{\mathrm{d}t}\int_V \mathbf{v}\rho \mathrm{d}V = \int_S \mathbf{t}_n \mathrm{d}S + \int_V \mathbf{f}\rho \mathrm{d}V \tag{2}$$

$$\frac{\mathrm{d}}{\mathrm{d}t}\int_V \mathbf{r}\times\mathbf{v}\rho \mathrm{d}V = \int_S (\mathbf{r}\times\mathbf{t}_n + \mathbf{m}_n)\mathrm{d}S + \int_V (\mathbf{r}\times\mathbf{f} + \mathbf{c})\rho \mathrm{d}V \tag{3}$$

$$\frac{\mathrm{d}}{\mathrm{d}t}\int (\tfrac{1}{2}\mathbf{v}\cdot\mathbf{v} + U)\rho \mathrm{d}V = \int_S (\mathbf{t}_n\cdot\mathbf{v} + \tfrac{1}{2}\mathbf{m}_n\cdot\nabla\times\mathbf{v})\mathrm{d}S + \int_V (\mathbf{f}\cdot\mathbf{v} + \tfrac{1}{2}\mathbf{c}\cdot\nabla\times\mathbf{v})\rho \mathrm{d}V \tag{4}$$

where $\mathrm{d}/\mathrm{d}t$ is the material time-derivative, ρ the mass density, $\mathbf{r}$ the spatial position vector from a fixed origin, $\mathbf{v}$ $(= \mathrm{d}\mathbf{r}/\mathrm{d}t)$ the material velocity, U the internal energy per unit mass, $\nabla = \partial/\partial\mathbf{r}$,

and $\frac{1}{2}\nabla \times \mathbf{v}$ the vorticity. The usual force-stress dyadic $\boldsymbol{\tau}$ and the couple-stress dyadic $\boldsymbol{\mu}$ are defined as follows:

$$\mathbf{t}_n = \mathbf{n}\cdot\boldsymbol{\tau} \text{ and } \mathbf{m}_n = \mathbf{n}\cdot\boldsymbol{\mu} \tag{5}$$

Applying the divergence theorem to Equations 1, 2, 3, 4, together with 5, the Cosserat equations are obtained:

$$\nabla\cdot\boldsymbol{\tau} + \rho\mathbf{f} = \rho\,\dot{\mathbf{v}} \tag{6}$$

$$\nabla\cdot\boldsymbol{\mu} + \rho\mathbf{c} + \boldsymbol{\tau}_{\times}\mathbf{I} = 0 \tag{7}$$

$$\nabla\cdot\boldsymbol{\tau}^S + \tfrac{1}{2}\nabla\times\nabla\cdot\boldsymbol{\mu} + \rho\mathbf{f} + \tfrac{1}{2}\nabla\times\rho\mathbf{c} = \rho\dot{\mathbf{v}} \tag{8}$$

$$\rho\dot{U} = \boldsymbol{\tau}^S : \nabla\mathbf{v} + \tfrac{1}{2}\boldsymbol{\mu} : \nabla\nabla\times\mathbf{v} \tag{9}$$

where $\dot{\mathbf{v}} = d\mathbf{v}/dt$, $\mathbf{I} \equiv \nabla\mathbf{r}$, and $\boldsymbol{\tau}^S$ is the symmetric part of $\boldsymbol{\tau}$. Equations 8 and 9 may be rewritten, respectively, as:

$$\nabla\cdot\boldsymbol{\tau}^S + \tfrac{1}{2}\nabla\times\nabla\cdot\boldsymbol{\mu}^D + \rho\mathbf{f} + \tfrac{1}{2}\nabla\times\rho\mathbf{c} = \rho\dot{\mathbf{v}} \tag{10}$$

$$\rho\dot{U} = \boldsymbol{\tau}^S : \nabla\mathbf{v} + \tfrac{1}{2}\boldsymbol{\mu}^D : \nabla\nabla\times\mathbf{v} \tag{11}$$

where $\boldsymbol{\mu}^D$ is the deviator of $\boldsymbol{\mu}$:

$$\boldsymbol{\mu}^D = \boldsymbol{\mu} - \tfrac{1}{3}\boldsymbol{\mu}:\mathbf{II} \tag{12}$$

Since the scalar of the couple-stress and the antisymmetric part of the force-stress are left indeterminate in the Cosserat theory, it is an incomplete theory but more tractable, in contrast to the more extended theories such as the double-stress theory [35, 36], strain-gradient theory, or theory of microelasticity.

3.1.2. Linearization

When linearized, Toupin's equation [32] for the specific internal energy W can be expressed in terms of the following variables:

$$\boldsymbol{\varepsilon} \equiv \tfrac{1}{2}(\nabla\mathbf{u} + \mathbf{u}\nabla) \text{ and } \boldsymbol{\kappa} = \tfrac{1}{2}\nabla\nabla\times\mathbf{u} \tag{13}$$

That is,

$$\rho_0 U \equiv W = \tfrac{1}{2}\boldsymbol{\kappa}:\boldsymbol{a}:\boldsymbol{\kappa} + \boldsymbol{\varepsilon}:\boldsymbol{b}:\boldsymbol{\kappa} + \tfrac{1}{2}\boldsymbol{\varepsilon}:\boldsymbol{c}:\boldsymbol{\varepsilon} \tag{14}$$

From this, the linearized forms of Toupin's constitutive equations result:

$$\boldsymbol{\tau}^S = \frac{\partial W}{\partial \boldsymbol{\varepsilon}} = \boldsymbol{c}:\boldsymbol{\varepsilon} + \boldsymbol{b}:\boldsymbol{\kappa} \tag{15}$$

$$\boldsymbol{\mu}^D = \frac{\partial W}{\partial \boldsymbol{\kappa}} = \boldsymbol{\varepsilon}:\boldsymbol{b} + \boldsymbol{\kappa}:\boldsymbol{a} \tag{16}$$

For the triclinic system (most anisotropic), there are 36 independent components of $\boldsymbol{a}$, 48 independent components of $\boldsymbol{b}$, and the usual 21 independent components of $\boldsymbol{c}$, each of the three being tetradic. However, the internal energy-density of an isotropic material has a much simplified form:

$$W = 2\eta\,\boldsymbol{\kappa}:\boldsymbol{\kappa} + 2\eta'\boldsymbol{\kappa}:\boldsymbol{\kappa}_c + \tfrac{1}{2}\lambda\varepsilon_S^2 + \mu\boldsymbol{\varepsilon}:\boldsymbol{\varepsilon} \tag{17}$$

from which

$$\begin{aligned}\boldsymbol{\tau}^S &= \lambda\varepsilon_S\mathbf{I} + 2\mu\boldsymbol{\varepsilon}\\ \boldsymbol{\mu}^D &= 4\eta\boldsymbol{\kappa} + 4\eta'\boldsymbol{\kappa}_c\end{aligned} \tag{18}$$

where λ and μ are Lamé's constants; η and η' the couple-stress constants; $\boldsymbol{\kappa}_c$ the conjugate of $\boldsymbol{\kappa}$; and ε_S the scalar of $\boldsymbol{\varepsilon}$. In other words, there are only the four independent constants for the isotropic medium.

3.1.3. Wave motion

When Equations 13 and 18 are inserted in Equation 10, the displacement-equation of motion is obtained:

$$\mu\nabla^2\mathbf{u} + (\lambda+\mu)\nabla\nabla\cdot\mathbf{u} + \eta\nabla^2\nabla\times\nabla\times\mathbf{u} + \rho\mathbf{f} + \tfrac{1}{2}\rho\nabla\times\mathbf{c} = \rho\ddot{\mathbf{u}} \tag{19}$$

where $\ddot{\mathbf{u}} = \partial^2\mathbf{u}/\partial t^2$. Note that η' does not appear in Equation 19. In the absence of body-force and body-couple, Equation 19 becomes:

$$\mu\nabla^2\mathbf{u} + (\lambda+\mu)\nabla\nabla\cdot\mathbf{u} + \eta\nabla^2\nabla\times\nabla\times\mathbf{u} = \rho\ddot{\mathbf{u}} \tag{20}$$

Taking the divergence and curl of Equation 20, the following equations are obtained, respectively,

$$c_1^2\nabla^2\nabla\cdot\mathbf{u} = \nabla\cdot\ddot{\mathbf{u}} \tag{21}$$

$$c_2^2(1 - l^2\nabla^2)\nabla^2\,\nabla\times\mathbf{u} = \nabla\times\ddot{\mathbf{u}} \tag{22}$$

where

$$\begin{aligned}l^2 &= \eta/\mu\\ c_1^2 &= (\lambda+2\mu)/\rho\\ c_2^2 &= \mu/\rho.\end{aligned} \tag{23}$$

Thus, the dilatation is propagated non-dispersively, with velocity c_1, as it is without couple-stresses. However, propagation of the rotation is influenced by couple-stresses. For the plane wave, e.g.

$$\begin{aligned}\nabla\times\mathbf{u} &= \mathbf{d}A\exp[i\xi(\mathbf{n}\cdot\mathbf{r} - ct)]\\ &= \mathbf{d}A\exp[i(\xi\mathbf{n}\cdot\mathbf{r} - \omega t)]\end{aligned} \tag{24}$$

where **d** is a unit vector, A the amplitude, ξ the wave number, **n** the unit wave normal, c the phase velocity, and ω the circular frequency. Substituting Equation 24 in Equation 22, the following equations are obtained:

$$\begin{aligned} c^2 &= c_2^2(1 + l^2\xi^2) \\ \omega^2 &= \xi^2 c_2^2(1 + l^2\xi^2) \end{aligned} \tag{25}$$

the latter giving the two roots for ξ^2:

$$\begin{aligned} \xi_1^2 &= \tfrac{1}{2}l^{-2}[(1 + 4l^2\omega^2/c_2^2)^{1/2} - 1] \\ \xi_2^2 &= -\tfrac{1}{2}l^{-2}[(1 + 4l^2\omega^2/c_2^2)^{1/2} + 1] \end{aligned} \tag{26}$$

Since l is known to be real, there are two dispersive rotational waves: one propagating and the other non-propagating. The group velocity of the real wave,

$$\frac{d\omega}{d\xi_1} = c_2(1 + 2l^2\xi_1^2)/(1 + l^2\xi_1^2)^{1/2} \tag{27}$$

increases monotonically with increasing $\xi_1 l$. This increase might produce a detectable effect of couple-stress in high-frequency vibrations. If $\xi_1 l$ is small, i.e. if the wavelength is large in comparison with the material constant l, the group velocity is approximately the same (c_2) as it would be without couple-stresses.

3.2. Linear elastic microstructure theory [15].

Here, Mindlin's tensor notation will be used in order to avoid introducing a new system of symbols.

3.2.1. Kinematics and definitions

For a material volume V, bounded by a surface S, let $X_i (i = 1,2,3)$ be the rectangular Cartesian components of the material position vector measured from a fixed origin, and x_i the components of the spatial position vector in the same rectangular frame. The components of (macro)displacement of a material particle are defined as

$$u_i \equiv x_i - X_i \tag{28}$$

Embedded in each material particle there is assumed to be a microvolume V' in which X_i' and x_i' are the components of the material and spatial position vectors, respectively, referred to axes parallel to those of the x_i, with origin fixed in the particle. Therefore, the origin of the coordinates x_i' moves with displacement u_i. The components of micro-displacement are defined as

$$u_i' \equiv x_i' - X_i' \tag{29}$$

The absolute values of the displacement-gradients are assumed to be small in comparison with unity so that we may write

$$\frac{\partial u_j}{\partial X_i} \approx \frac{\partial u_j}{\partial x_i} \equiv \partial_i u_j ; u_j = u_j(x_i, t) \tag{30}$$

$$\frac{\partial u_j'}{\partial X_i'} \approx \frac{\partial u_j'}{\partial x_i'} \equiv \partial_i' u_j' ; \; u_j' = u_j'(x_i, x_i', t) \tag{31}$$

where t is the time. Also assume that the micro-displacement can be expressed as a sum of products of specified functions of the x_i' and arbitrary functions of the x_i and t. In a linear approximation, only a single term of the series is retained:

$$u_j' = x_k' \psi_{kj} ; \psi_{kj} = \psi_{kj}(x_i, t) \tag{32}$$

then the displacement-gradient or microdeformation is

$$\partial_i' u_j' = \psi_{ij} \tag{33}$$

which is taken to be homogeneous in the micro-medium V' and inhomogeneous in the macro-medium V. The symmetric part of ψ_{ij} is micro-strain:

$$\psi_{(ij)} \equiv \tfrac{1}{2}(\psi_{ij} + \psi_{ji}) \tag{34}$$

and the antisymmetric part is the microrotation:

$$\psi_{[ij]} \equiv \tfrac{1}{2}(\psi_{ij} - \psi_{ji}) \tag{35}$$

From these definitions, the following three quantities are defined: the usual strain (or the macro-strain), a relative deformation and a micro-deformation (macrogradient of the microdeformation), respectively,

$$\epsilon_{ij} \equiv \tfrac{1}{2}(\partial_i u_j + \partial_j u_i) \tag{36}$$

$$\gamma_{ij} \equiv \partial_i u_j - \psi_{ij} \tag{37}$$

$$\kappa_{ijk} \equiv \partial_i \psi_{jk} \tag{38}$$

For the potential energy-density (potential energy per unit macrovolume), W, assume that W is a function of the forty-two variables ϵ_{ij}, γ_{ij} and κ_{ijk}:

$$W = W(\epsilon_{ij}, \gamma_{ij}, \kappa_{ijk}) \tag{39}$$

Then, the Cauchy stress τ_{ij}, the relative stress σ_{ij} and the double stress μ_{ijk} are defined as follows:

$$\tau_{ij} \equiv \frac{\partial W}{\partial \epsilon_{ij}} = \tau_{ji} \tag{40}$$

$$\sigma_{ij} \equiv \frac{\partial W}{\partial \gamma_{ij}} \tag{41}$$

$$\mu_{ijk} \equiv \frac{\partial W}{\partial \kappa_{ijk}} \tag{42}$$

3.2.2. Stress-equations of motion and constitutive equations

Let f_j be the body-force per unit volume, t_j the surface-force per unit area (stress vector or traction), ϕ_{jk} the double force per unit volume, and T_{jk} the double force per unit area. From the variational equation of motion [15], then follow the twelve stress-equations of motion:

$$\partial_i(\tau_{ij} + \sigma_{ij}) + f_j = \rho \ddot{u}_j \tag{43}$$

$$\partial_i \mu_{ijk} + \sigma_{jk} + \Phi_{jk} = \tfrac{1}{3}\rho' d_{ij}^2 \ddot{\psi}_{lk} \tag{44}$$

and the twelve traction boundary conditions:

$$t_j = n_i(\tau_{ij} + \sigma_{ij}) \tag{45}$$

$$T_{jk} = n_i \mu_{ijk} \tag{46}$$

where ρ' is the mass of micromaterial per unit macrovolume, and d_{ij}^2 is a linear combination of products of the edges d_i of a parallelepiped with the microvolume V'. The linear equations of a Cosserat continuum [4] are obtained by putting $\psi_{(ij)} = 0$. Then $\sigma_{(ij)} = \tau_{ij}$ and $\mu_{i(jk)} = 0$; and there remain $\mu_{i[jk]}$ (the Cosserat couple-stress) and $\sigma_{[ij]}$ (the antisymmetric part of an asymmetric stress τ_{ij}). However, in the present theory, the Cauchy stress τ_{ij} is symmetric and $\sigma_{[ij]}$ is the antisymmetric part of the asymmetric relative stress σ_{ij}.

For potential energy-density a homogeneous, quadratic function of the forty-two variables $\epsilon_{ij}, \gamma_{ij}, \kappa_{ijk}$, is taken to be

$$\begin{aligned} W = {} & \tfrac{1}{2} c_{ijkl} \epsilon_{ij} \epsilon_{kl} + \tfrac{1}{2} b_{ijkl} \gamma_{ij} \gamma_{kl} \cdot \\ & + \tfrac{1}{2} a_{ijklmn} \kappa_{ijk} \kappa_{lmn} + d_{ijklm} \gamma_{ij} \kappa_{klm} \\ & + f_{ijklm} \kappa_{ijk} \epsilon_{lm} + g_{ijkl} \gamma_{ij} \epsilon_{kl} \end{aligned} \tag{47}$$

Only 903 of the 1764 coefficients in Equation 47 are independent. From Equation 47 together with Equations 40, 41 and 42, the following constitutive equations are obtained for the most anisotropic material:

$$\tau_{pq} = c_{pqij} \epsilon_{ij} + g_{ijpq} \gamma_{ij} + g_{ijkpq} \kappa_{ijk} \tag{48}$$

$$\sigma_{pq} = g_{pqij} \epsilon_{ij} + b_{ijpq} \gamma_{ij} + d_{pqijk} \kappa_{ijk} \tag{49}$$

$$\mu_{pqr} = f_{pqrij} \epsilon_{ij} + d_{ijpqr} \gamma_{ij} + a_{pqrijk} \kappa_{ijk} \tag{50}$$

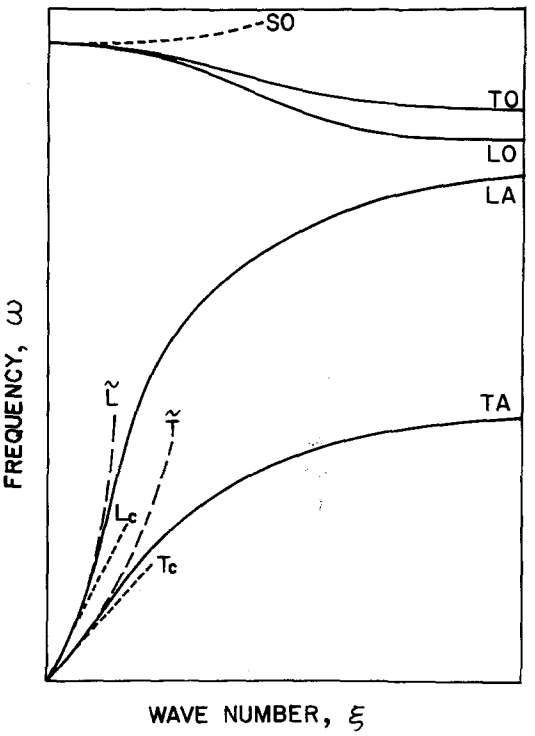

Figure 1 Sketch of possible configuration of real branches of dispersion curves. LA = longitudinal acoustical; TA = transverse acoustical; SO = shear optical; TO = transverse optical; LO = longitudinal optical; $\tilde{L}$, $\tilde{T}$ = low frequency approximation; L_c, T_c = classical elasticity.

In the case of an isotropic material the number of independent coefficients is reduced to only 18.

3.2.3. Plane wave propagation for long wavelengths

By substituting plane wave solutions, for example, of the types

$$u_i = u_i(x_1, t) \text{ and } \psi_{ij} = \psi_{ij}(x_1, t) \tag{51}$$

in the displacement-equations of motion for an isotropic material [15], it has been found that there exist eight branches of real waves in the dispersion curves of frequency against wave number. That is, the six optical branches: shear optical (SO), rotational optical (RO), longitudinal optical (LO), longitudinal dilatational optical (LDO), transverse optical (TO), and trasverse rotational optical (TRO); and the two acoustical branches: longitudinal acoustical (LA) and transverse acoustical (TA). SO, TA, TO and TRO are degenerate. In Fig. 1 only the acoustical branches and three lower optical branches are shown together with the corresponding branches

TABLE I Frequency dependence of the ultrasonic velocities in PMMA at 22.2° C [49]

Frequency (MHz)	Longitudinal (km sec^{-1})	Shear (km sec^{-1})
6	2.7564	1.4015
10	2.7605	1.4048
18	2.7642	1.4051
20	2.7651	1.4057
30	2.7655	1.4061

of low frequency approximation and of classical elasticity.

4. Discussion

Based on Cauchy's theory on the dispersion of light (1830) [41], Powell (1841) computed the velocity V of a wave propagating along one axis of a cubic lattice structure as a function of wavelength λ with point masses spaced a from one another. V is given by

$$V = V_\infty \frac{|\sin(\pi a/\lambda)|}{\pi a/\lambda} \tag{52}$$

where V_∞ is the velocity for infinite wavelength [42]. However, Powell failed to consider the frequency as a function of the wavelength. The curve of velocity against reciprocal wavelength appears to be perfectly normal at the point $\lambda = 2a$; not so, however, for the frequency f against reciprocal wavelength, as noted by Kelvin (1883) [43]. The angular frequency $\omega(= 2\pi f)$ as a function of the magnitude of the wave vector, k, turns out to be

$$\omega(k) = C|\sin \tfrac{1}{2}ka|, \tag{53}$$

where C is a constant that is a function of the force constant and the mass. Equation 53 shows that $\omega(k)$ is a straight line for small values of k, i.e. large values of wavelength, which is in agreement with the earlier calculations. The values of k must be limited to the range

$$-\frac{\pi}{a} \leqslant k \leqslant \frac{\pi}{a} \tag{54}$$

in order to remove the ambiguity that for a given frequency the wavelength is not completely determined. Born and Kármán (1912) investigated the propagation of waves in crystals and rediscovered Kelvin's analysis [44]. Brillouin (1946) summarized these investigations, together with his own contributions, in his book [45].

When acoustic waves are propagated in a fibre-reinforced viscoelastic composite material, they are dispersed by two distinct mechanisms, viscoelastic and geometric dispersions. The geometric dispersion is expressed by Equations 53 and 54 in which the interfibre spacing corresponds to the distance of point masses or atomic spacing. In other words, it is characterized by the existence of passbands and forbidden bands, and by a wave-filtering phenomenon, in addition to the constant group or phase velocity for long wavelengths. In the viscoelastic dispersion, on the other hand, the phase (or group) velocity increases with increasing frequency, approaching a plateau at high frequencies, and together with the characteristic frequency dependence of attenuation [46, 47].

Sutherland and Lingle [48] investigated geometric dispersion by measuring the phase velocity and attenuation in the elastic fibrous composites of Al–W (2.2 and 22.1% W by volume), showing that the phase velocity V_p decreases with increasing frequency f within each passband, e.g. $V_p = 5.99$ to 5.42 km sec^{-1} for $f = 0.63$ to 3.57 MHz in a 2.2 mol% W–Al composite. Table I shows the ultrasonic velocities in PMMA at 22.2° C in the frequency range from 6 to 30 MHz, reported by Asay *et al.* [49]. PMMA is a typical viscoelastic solid. The relative increases of longitudinal and shear velocities in this frequency range (24 MHz) are only 0.33% in both cases. Sutherland [50] also tried to separate geometric and viscoleastic dispersions in two fibre-reinforced viscoelastic

TABLE II Measured phase and group velocities in the human skull (diploe) [51]

Frequency (MHz)	Phase velocity (km sec^{-1})	Group velocity (km sec^{-1})
0.5	2.19	2.84
1.5	2.53	2.81
3.0	3.87	3.11
Relative change (%)	24	28

TABLE IIIA Frequency dependence of the ultrasonic velocities in the human femur at room temperature; longitudinal velocity (km sec^{-1})

Mode	Propagation direction, N	Displacement direction, U	Frequency (MHz)			Relative change (%)
			2	5	10	
αL	[0 0 1]	[0 0 1]	4.18	4.24	4.30	2.8
γL	[1 0 0]	[1 0 0]	3.36	3.50	3.72	9.7
45L	$[1/\sqrt{2}\ 0\ 1/\sqrt{2}]$	$\sim [1/\sqrt{2}\ 0\ 1/\sqrt{2}]$	3.84	3.87	3.95	2.8

TABLE IIIB Frequency dependence of the ultrasonic velocities in the human femur at room temperature; transverse velocity (km sec^{-1})

Mode	Propagation direction, N	Displacement direction, U	Frequency (MHz)			Relative change (%)
			1	2	5	
αT	[0 0 1]	[1 0 0]	1.98	2.03	2.15	7.9
γT_h	[1 0 0]	[0 1 0]	1.85	1.84	1.98	6.6
γT_3	[1 0 0]	[0 0 1]	2.02	2.06	2.17	6.9
$45T_h$	$[1/\sqrt{2}\ 0\ 1/\sqrt{2}]$	[0 1 0]	1.87	1.96	2.06	9.2
$45T_v$	$[1/\sqrt{2}\ 0\ 1/\sqrt{2}]$	$\sim [-1/\sqrt{2}\ 0\ 1/\sqrt{2}]$	2.14	2.16	2.24	4.5

materials, a cloth-laminate quartz phenolic and stainless steel wires embedded in an Epon 828-Z matrix, finding that the viscoelastic contribution in these composites is small.

Table II shows the measured phase and group velocities (longitudinal) in the human skull (diploe) in the frequency range from 500 kHz to 3 MHz by Fry and Barger [51]. The relative changes in phase and group velocities are 24 and 28%, respectively, in this small frequency range (3.5 MHz). However, these authors have not given any explanation of the dispersion for diploe.

We have also reported on the frequency dependence of the ultrasonic velocities in human femoral cortical bone along eight unique orientations, employing a pulse through-transmission technique, as shown in Table III [52]. The respective relative velocity changes for the covered frequency ranges are given in the last column. The frequency range for longitudinal velocity measurements was from 2 to 10 MHz, whereas the transverse velocity measurements were done for the range from 1 to 5 MHz. In addition, our unpublished work shows that the frequency dependence of the ultrasonic velocities in polystyrene is negligible, with the same experimental set-up as for the human femur, in the frequency range of 2 to 20 MHz for longitudinal waves and of 1 to 10 MHz for transverse waves. Although the frequency dependence of the ultrasonic velocities for the femur is not as large as that for the skull, it is still too large in the narrow frequency ranges compared to that for PMMA. This suggests that there may be another dispersion mechanism involved in addition to the viscoelastic contribution. Previously [52], we have tried to attribute this frequency dependence for the human femur to viscoelastic effects alone, though unsatisfactorily.

The linear couple-stress theory [11] has been found to be reasonably satisfactory in explaining the torsion data on human compact bone [12–14], as mentioned previously. However, this theory shows, for an isotropic medium, that only the rotational waves are dispersive, whereas the dilatational wave is not influenced by couple-stresses. In contrast, the more generalized continuum theories (e.g. Mindlin's structured Cosserat theory [15]) indicate that both the longitudinal and transverse velocities (acoustical branches) increase with increasing wave number (or frequency), even in its low frequency approximations, see Fig. 1, which is consistent with the preliminary studies on bone.

Acknowledgement

This work was supported by the Whitaker Foundation, and USPHS through NIDR Training Grant No. 5 T32-DEORO5405 at Rensselaer Polytechnic Institute.

References

1. G. SINES and J. L. WAISMAN (eds), "Metal Fatigue" (McGraw-Hill, New York, 1959) p. 293.
2. N. J. PETCH, *J. Iron Steel Inst. (London)* **174** (1953) 25.
3. *Idem, Phil. Mag.* **1** (1956) 186.

4. E. COSSERAT and F. COSSERAT, "Théorie des Corps Déformables" (Hermann, Paris, 1909).
5. R. D. MINDLIN, *Exp. Mech.* **3** (1963) 1.
6. W. T. KOITER, *Proc. Koninkl. Nederl. Akad. Wetensch.* **67B** (1964) 17.
7. J. SCHIJVE, *J. Mech. Phys. Solids* **14** (1966) 113.
8. R. W. ELLIS and C. W. SMITH, *Exp. Mech.* **7** (1967) 372.
9. R. D. GAUTHIER and W. E. JAHSMAN, *J. Appl. Mech.* **42** (1975) 369.
10. R. W. PERKINS, JR and D. THOMPSON, *AIAA J.* **11** (1973) 1053.
11. R. D. MINDLIN and H. F. TIERSTEN, *Arch. Rat. Mech. Anal.* **11** (1962) 415.
12. J. F. C. YANG and R. S. LAKES, *Trans. ASME (J. Biomech. Eng.)* **103** (1981) 275.
13. R. S. LAKES, *ibid.* **104** (1982) 6.
14. J. F. C. YANG and R. S. LAKES, *J. Biomech.* **15** (1982) 91.
15. R. D. MINDLIN, *Arch. Rat. Mech. Anal.* **16** (1964) 51.
16. V. R. PARFITT and A. C. ERINGEN, *J. Acoust. Soc. Amer.* **45** (1969) 1258.
17. S. D. POISSON, *Mém. Acad. Sci.* **18** (1842) 3.
18. *Idem, Compt. Rend.* **9** (1839) 517.
19. A. L. CAUCHY, *ibid.* **32** (1851) 323.
20. W. VOIGT, *Abh. K. Ges. Wiss. z. Göttingen (Math. Cl.)* **34** (1887) 1.
21. *Idem, Nachr. K. Ges. Wiss. z. Göttingen (Math. – phys. Kl.)* **1894[2]** (1894) 72 (often misquoted as *Gött. Abh.*).
22. P. DUHEM, *Ann. École Norm. (3)* **10** (1893) 183.
23. E. REISSNER, *J. Math. & Phys.* **23** (1944) 192.
24. J. L. ERICKSEN and C. TRUESDELL, *Arch. Rat. Mech. Anal.* **1** (1958) 295.
25. W. GÜNTHER, *Abh. Braunschweigische Wiss. Ges.* **10** (1958) 195.
26. E. S. RAJAGOPAL, *Ann. Physik* **6** (1960) 12.
27. S. FLÜGGE (ed), "Handbuch der Physik", Vol. III/1 (Springer, Berlin, Göttingen, Heidelberg, 1960) p. 226.
28. E. L. AERO and E. V. KUVSHINSKII, *Fizika Tverdogo Tela* **2** (1960) 1399 [*Sov. Phys. Solid State* **2** (1961) 1272].
29. G. GRIOLI, *Ann. di Mat. Pura ed Appl. (Ser. 4)* **50** (1960) 389.
30. R. A. TOUPIN, *Arch. Rat. Mech. Anal.* **17** (1964) 85.
31. M. SCHÄFER (ed), "Miszellaneen der angewandten Mechanik" (Akademie, Berlin, 1962) p. 277.
32. R. A. TOUPIN, *Arch. Rat. Mech. Anal.* **11** (1962) 385.
33. A. C. ERINGEN and E. S. SUHUBI, *Int. J. Eng. Sci.* **2** (1964) 189.
34. E. S. SUHUBI and A. C. ERINGEN, *ibid.* **2** (1964) 389.
35. A. E. GREEN and R. S. RIVLIN, *Arch. Rat. Mech. Anal.* **16** (1964) 325.
36. *Idem, ibid.* **17** (1964) 113.
37. G. HERRMANN (ed), "R. D. Mindlin and Applied Mechanics" (Pergamon, New York, Oxford, 1974) p. 67.
38. H. LIEBOWITZ (ed), "Fracture", Vol. 2 (Academic Press, New York, London, 1968) p. 621.
39. C. E. WEATHERBURN, "Advanced Vector Analysis" (Bell, London, 1924).
40. J. W. GIBBS and E. B. WILSON, "Vector Analysis" (Dover, New York, 1960).
41. A. L. CAUCHY, *Bull. Sci. Math.* **14** (1830) 6.
42. B. POWELL (Rev.), "A General and Elementary View of the Undulatory Theory, as Applied to the Dispersion of Light" (Parker, London, 1841).
43. LORD KELVIN (W. THOMSON), *Proc. Roy. Inst.* **10** (1884) 185: also in "Popular Lectures and Addresses", Vol. 1 (Macmillan, London, New York, 1891) p. 154.
44. M. BORN and T. V. KÁRMÁN, *Phys. Z.* **13** (1912) 297.
45. L. BRILLOUIN, "Wave Propagation in Periodic Structures", 2nd edn (Dover, New York, 1953).
46. B. GROSS, "Mathematical Structure of the Theories of Viscoelasticity" (Hermann, Paris, 1953).
47. N. DAVIDS (ed), "International Symposium on Stress Wave Propagation in Materials" (Interscience, New York, 1960) p. 59.
48. H. J. SUTHERLAND and R. LINGLE, *J. Compos. Mater.* **6** (1972) 490.
49. J. R. ASAY, D. L. LAMBERSON and A. H. GUENTHER, *J. Appl. Phys.* **40** (1969) 1768.
50. H. J. SUTHERLAND, *Int. J. Solids Struc.* **11** (1975) 233.
51. F. J. FRY and J. E. BARGER, *J. Acoust. Soc. Amer.* **63** (1978) 1576.
52. H. S. YOON and J. L. KATZ, in "1976 Ultrasonics Symposium on Ultrasonics", edited by J. de Klerk and B. McAvoy (Institute of Electrical and Electronics Engineers, New York, 1976) p. 48.

Received 1 September
and accepted 20 September 1982